

Rosella: A Self-Driving Distributed Scheduler for Heterogeneous Clusters

Qiong Wu*, Zhenming Liu*

*College of William and Mary

ABSTRACT

Large-scale interactive web services and advanced AI applications make sophisticated decisions in real-time, based on executing a massive amount of computation tasks on thousands of servers. Task schedulers, which often operate in heterogeneous and volatile environments, require high throughput, i.e., scheduling millions of tasks per second, and low latency, i.e., incurring minimal scheduling delays for millisecond-level tasks. Scheduling is further complicated by other users' workloads in a shared system, other background activities, and the diverse hardware configurations inside datacenters.

We present Rosella, a new self-driving, distributed approach for task scheduling in heterogeneous clusters. Our system automatically *learns* the compute environment and *adjusts its scheduling policy* in real-time. The solution provides high throughput and low latency simultaneously, because it runs in parallel on multiple machines with minimum coordination and only performs simple operations for each scheduling decision. Our learning module monitors total system load, and uses the information to dynamically determine optimal estimation strategy for the backends' compute-power. Our scheduling policy generalizes power-of-two-choice algorithms to handle heterogeneous workers, reducing the max queue length of $O(\log n)$ obtained by prior algorithms to $O(\log \log n)$. We implement a Rosella prototype and evaluate it with a variety of workloads. Experimental results show that Rosella significantly reduces task response times, and adapts to environment changes quickly.

1. INTRODUCTION

Recent explosion of artificial intelligence and machine learning significantly altered the compute workloads in backend data centers. Users today expect real-time delivery of highly intelligent services to their devices. Search engines continuously predict search queries and refresh search results on browsers within a few tens of milliseconds, requiring processing of enormous tiny tasks on thousands of machines [1, 2]. Virtual and augmented reality devices continuously analyze video and render graphics based on the analysis results. The emerging class of advanced artificial intelligence (AI) applications (e.g., autonomous vehicles and

robotics) based on reinforcement learning need to perform many simulations (e.g., using Monte Carlo tree searches) in strict timing requirements, to determine the next action when interacting with physical or virtual environments [3].

It becomes prohibitively expensive to process such workloads in dedicated compute clusters. A single dedicated GPU-server costing \$2,000/month can process only one or two video streams [4], yet consumer products or surveillance solutions require analyzing thousands of data-streams simultaneously. Therefore, recent data-intense systems often attempt to tap in highly volatile, lower cost computing sources. For example, AWS leases under-utilized boxes at significantly reduced cost through the T instances, or spot instance bidding [5, 6], and research groups in large organizations share computing infrastructure.

The new design paradigm poses remarkable performance challenges for task schedulers to support these applications at scale:

High-throughput and low latency requirement. Task schedulers are now required to provide high throughput as they need to schedule millions of tasks per second for these applications [7]. At the same time, the scheduling needs to be low latency because the tasks are at millisecond level.

Heterogeneous environments. Task schedulers operate in environments composed of CPUs, GPUs, FPGAs, and specialized ASICs. Administrators may rent servers from public clouds (AWS, Azure, etc.) and markets (AWS marketplace). Different types of servers may be rented to minimize their changing prices and cost efficacies. Organizations using private clouds may host servers of different generations to postpone server upgrades and replacements at the same time.

Advanced cross-platform machine learning frameworks also accelerate the usage of heterogeneous boxes. tensorflow (a deep learning framework [8]) programs can be executed on smartphones, consumer-grade PCs, high-end GPUs, and other devices.

Unknown and evolving compute-power. Workers' performances are often time-varying in practice. For example, multiple groups in a large organization share the same clusters (see Figure 2). Each group wants to control its own scheduler, but each scheduler may not have full control over

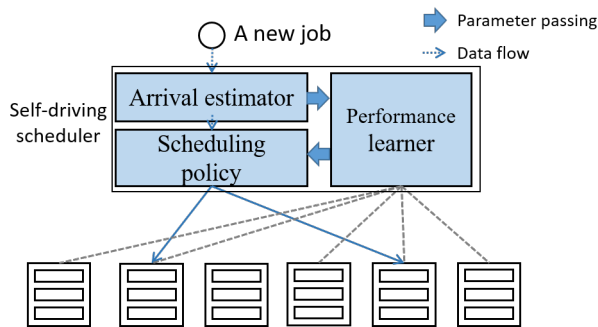


Figure 1: The architecture of Rosella: it continuously learns backend workers’ performance and adjusts its scheduling policy.

the workers it manages [9]. The compute-power of servers controlled by a different group’s scheduler may drop when an adjacent group launches a large batch of jobs. For public clouds, a similar challenge arises in managing volatile computing instances. For example, T instances offered by AWS come from residual/under-utilized resources, and the compute-throughputs fluctuate [6].

Our problem and contributions. A robust scheduler for heterogeneous systems in modern data centers must be *self-driving*, able to continuously adjust its policy as the workers’ compute power fluctuates. We consider the problem of designing a high-throughput and low-latency self-driving scheduler that simultaneously learns the workers’ processing power and act on the learned parameters. Our scheduler, coined as Rosella, possesses the following salient features (see also Figure 1):

1. *Efficiently learning the parameters.* Our system efficiently estimates the processing power of each worker. Our algorithm’s learning-time scales inverse-proportional to the load ratio, and logarithmically to the number m of servers. Both dependencies are essentially optimal, making the scheduler highly scalable. For example, when the number of servers doubles, learning time only increases by a constant unit of times.

2. *Heterogeneity-aware schedulers.* We unify two major scheduling techniques in our job-allocation algorithm. The first is the so-called *proportional sampling strategy* [10]. When a new task arrives, the scheduler chooses a worker according to a multinomial distribution so that the probability that the i -th worker is chosen is proportional to its compute-power, e.g., if the i -th worker is five times faster than the j -th worker, the i -th worker is five times more likely to be chosen. The second is the so-called *power-of-two-choices* (PoT) strategy (see e.g., [11] and references therein). When a new task arrives, we execute the proportional sampling algorithm twice to obtain two candidate workers, and assigns the task to the worker with the shorter queue.

This algorithm reduces the worst-case queue length from $O(\log n)$ to $O(\log \log n)$, generalizing the standard

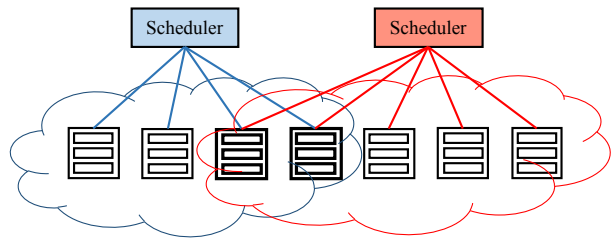


Figure 2: The demand for self-driving schedulers: two schedulers control two private clusters that are logically separate. But workers in different clusters may share the same physical servers (two bolded servers in the middle). Therefore, the workload of one cluster may affect the compute-throughput of another cluster.

power-of-two-choices result. Subtle and complex decisions need to be made in generalizing the PoT. For example, when we have a server that is 10 times as fast as an average server, a natural approach is to view the powerful server as a union of 10 servers (think of running 10 VMs in the fast server). This approach fails to work in our analysis.

2. BACKGROUND AND MOTIVATION

We consider a distributed system that consists of n workers/servers, each connected to a scheduler. Jobs arriving to the scheduler may contain one or more tasks. When a new job arrives, the scheduler can probe a certain number of workers and decide how the tasks should be assigned to the workers based on their queue length.

In a unit of time (say one minute), a total number of λ tasks arrive (λ is called arrival rate). Processing/compute power of the workers is heterogeneous. Worker i can process μ_i tasks on average in a unit of time (μ_i is called service rate).

Let $\mu = \sum_{i \leq n} \mu_i$ be the system’s total processing power, and $\alpha = \lambda/\mu$ be the system’s load ratio. Both μ_i and λ can change over time to reflect volatility in the system.

We aim to design a simple scheduling algorithm that simultaneously optimizes the following metrics:

1. *Response time.* When a job arrives, how much time does the system need to process the job? Another related metrics is the length of workers’ queues in the system.

2. *Learning and recovery time.* When a system starts up, or experiences a shock (many μ_i ’s changed), the scheduler does not have accurate estimates on μ_i ’s. How much time does the system need to re-learn the μ_i ’s, and once learned, how much time does the system need to recover (e.g., handling the backlogs produced by the scheduler using inaccurate/old estimates μ_i)?

2.1 Motivation: failures of prior algorithms

Our system needs to simultaneously learn the servers’ performance and schedule the jobs based on the estimation. Learning and scheduling algorithms have been widely studied, but none are directly applicable in our setting (see e.g.,

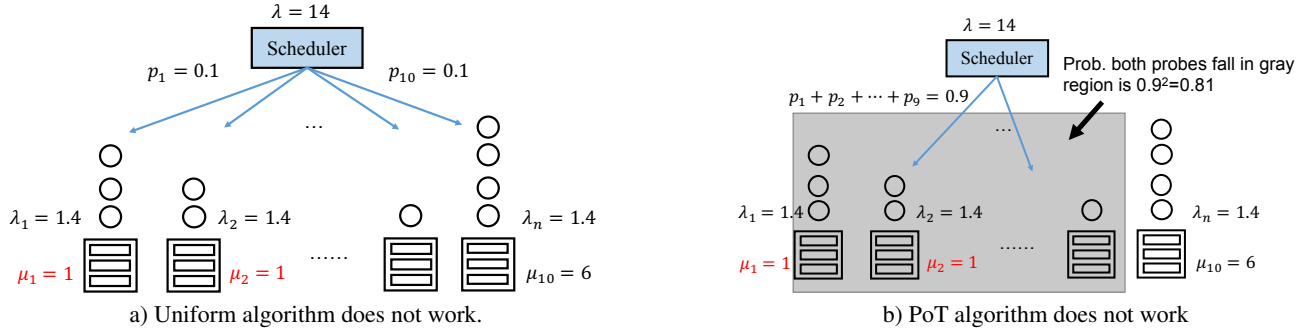


Figure 3: Both the uniform algorithm and PoT algorithm fail to work. There are 10 servers. $\mu_1 = \mu_2 = \dots = \mu_9 = 1$. $\mu_{10} = 6$. $\lambda = 14$. **Uniform algorithm (left): $\mu_1 = 1$ while $\lambda_1 = 1.4$, implying that in the long run, worker 1 is non-stationary. **PoT algorithm (right):** with probability 0.81, workers 1 to 9 receive a job. The aggregate arrival rate to workers 1 to 9 is $14 \times 0.81 = 11.34$, but the total processing rate of workers 1 to 9 is only 9, implying that in the long run workers 1 to 9 are non-stationary.**

[12, 11, 13, 14, 15, 16, 17]). Below, we review the commonly used scheduling algorithms and learning algorithms and explain why they are not applicable.

2.1.1 Scheduling algorithms

Uniform algorithm. In this algorithm, when a new job arrives, the scheduler uniformly chooses a worker to serve it (see, e.g., Section 5 of [18]). When all μ_i 's are uniform, the system consists of n independent standard queues. At each time unit, each queue receives λ/n tasks and can process μ/n tasks. All queues can process more tasks than they receive and thus all of them are stationary. The expected length of the largest queue is $O(\log n)$.

The uniform algorithm does not work when the service rates are different for different servers, i.e., by assigning the same amount of jobs to each server, the faster servers are underloaded and slower servers are overloaded. Some slower servers need to process more jobs than they can process. In long run, the length of their queues becomes unbounded.

EXAMPLE 1 (UNIFORM ALGORITHM DOES NOT WORK). See Figure 3a. There are 10 workers. The service rates for workers 1 to 9 are 1. The service rate for worker 10 is 6. The arrival rate of the jobs is 14. The uniform algorithm assigns 10% of jobs to worker 1 (i.e., $\lambda_1 = 1.4$) but $\mu_1 = 1$, implying that in the long run, worker 1 needs to process more tasks than its capacity.

Power of two choices (PoT). When a new task arrives, the scheduler probes two random workers and assigns the new job to the worker with shorter queue. The PoT algorithm has improved worst-case queue length when the workers are homogeneous i.e., with high probability the largest queue length is $O(\log \log n)$ (see e.g., [11]).

The PoT algorithm suffers the same problem (i.e., faster workers are underloaded and slower workers are overloaded).

EXAMPLE 2 (PoT DOES NOT WORK). See Figure 3b. Using the same configuration in Example 1, i.e., $\lambda = 14$, $\mu_1 = \dots = \mu_9 = 1$, and $\mu_{10} = 6$, with probability $0.9 \times 0.9 = 0.81$, the scheduler selects 2 slow workers so one of them will process the job. Thus, with probability 0.81, the new job uses a slow server. In one unit of time, on average there are $14 \times 0.81 = 11.34$ jobs arriving at the slow workers, but the slow workers' total processing power is only 9, implying that in the long run the slow workers need to process more jobs than their capacity (i.e., they are non-stationary).

Heterogeneity-Aware Load Balancing. Recent attempts to address the heterogeneity issue via assigning more jobs to more powerful workers (see e.g., [10]) have not been implemented and tested against realistic workloads. In addition, they impractically assume accurate knowledge of the servers' processing powers, and that the processing power does not change over time.

2.1.2 Learning algorithms

Explore-exploit paradigm. One reliable way to estimate μ_i is to compute the average processing time of the most recent tasks, so long as the tasks are sufficiently recent (so they reflect the worker's current performance). The explore-exploit paradigm arises because we do not want to assign many jobs to slow workers (i.e., exploit more powerful ones) and we also want to closely track the slower workers' processing power so that we can use it when it becomes faster (explore the weaker ones).

The explore-exploit paradigm has been widely studied (e.g., multi-arm bandit problems [19]), but the solutions only focus on the so-called regret bound, or the convergence rate to the ground-truth. In the regret analysis, in every round (when a job arrives in our setting), a cost occurs after the algorithm makes a decision (on assigning the jobs), and the cost, referred to as "regret", is a function of the difference between the ground-truth and our estimates. Regret analysis

assumes that the costs/regrets are memoryless, (i.e., a wrong decision is only penalized once). In our setting, a wrong decision may have a long-lasting effect (i.e., an adversarial impact on all subsequent load-balancing decisions). Thus, it is unclear whether regret minimization is the correct objective in our setting.

Our learning objective. Instead of minimizing the regret, our learning and schedule algorithm simultaneously must 1. *Efficiently learn the processing power.* When the system is cold-started, or has recently experienced a shock, the algorithm needs to efficiently (re)-learn the workers’ processing power; 2. *Rapidly converge to stationary distribution.* When the algorithm re-learns the workers’ processing power, the system rapidly converges to the stationary distribution (i.e., efficiently handles the backlogs from using inaccurate/old processing power estimates); and 3. *Be robust against estimation errors.* The scheduler must work well in the presence of small estimation error.

3. OVERVIEW OF THE ALGORITHM

This section explains Rosella’s architecture, and the operational details. Figure 1 shows the architecture and the three components:

1. **Arrival estimator.** This component estimates of the arrival rate λ of the system.
2. **Scheduling policy.** When a new job arrives, this component communicates with a constant number of workers (probes their states) and assigns the work with the shortest queue to the new job.
3. **Performance learner.** This component continuously estimate workers’ processing power (hereafter, also referred as *worker speed*).

Components’ interaction. When a job arrives, it goes to the arrival estimator, which estimates and updates the arrival rate λ of the system. Next, the job goes to the scheduling policy, which uses the estimates of μ_i provided by the performance learner to choose the appropriate worker.

The performance learning, which operates in the background, continuously maintain current estimates of each worker’s processing power. It takes the estimate λ as input and uses it to determine how to communicate with the workers.

Technical challenges.

1. *Power-of-two generalization.* Recall that a classical PoT algorithm uniformly samples two workers, and uses the one with lighter loads to process the new job. Generalization of the PoT algorithm requires us to use non-uniform sampling (see Sec. 3.1 for further discussions), and redefine the rule of choosing a worker because both of the two policies below are plausible (see e.g., [20, 21, 22, 23]):

1. The *join the shortest queue* policy (SQ(2)): assigns the incoming job to the queue with the shorter length.

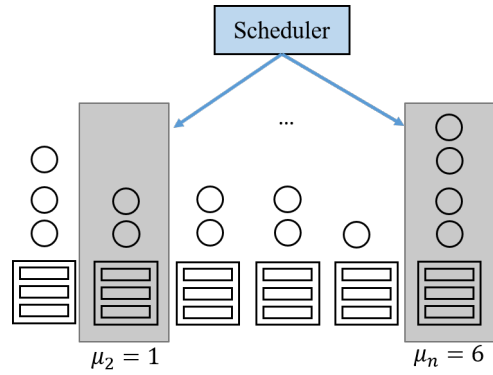


Figure 4: Generalizing PoT by using SQ(2) and/or LL(2) policies. The scheduler chooses two workers (gray boxes). The left worker has a shorter queue but its expected waiting time is longer (because it is slower). The SQ(2) policy chooses the left worker while the LL(2) policy chooses the right worker.

2. The *join the least loaded queue* policy (LL(2)): assigns the incoming job to the queue to the shorter waiting time.

Figure 4 presents an example. One candidate server has a shorter queue and a longer expected waiting time. The SQ(2) policy would chooses the one server with the shorter queue while the LL(2) policy would chooses the server with shorter waiting time. Section 3.1 discusses the behaviors of these policies and our design choice.

2. *The explore-exploit paradigm and more jobs are better.* Our performance learning component must balance the tradeoffs between estimating slow workers (that could potentially become fast) and assigning more jobs to fast workers. While this is a classical explore-exploit paradigm extensively studied in multi-arm bandit problems, one key difference here is that in multi-arm bandit problems, a scheduler need to passively perform the explore operations (e.g., only when a job arrives can the scheduler use it to explore) the workers’ performance; whereas our algorithm can actively explore servers’ performance by *creating new jobs*.

Optimizing the learning performance involves carefully controlling the number of jobs that need to be to be created for the purpose of exploration. Creating too few jobs will not accelerate the learning process, while creating too many jobs will slow down the whole system.

In what follows, we walk through each component in Rosella in details.

3.1 The scheduling policy

The scheduling policy component has access to estimates $\hat{\mu}_i$ from the performance learning component. It needs to determine worker to use when a new job arrives.

Our policy deviates from the classical PoT algorithms in two major ways (see also Figure 5 for the algorithm).

1. **Proportional sampling schedule (PSS).** To circumvent heterogeneity of the workers, our approach relies on the so-

called proportional sampling procedure that probes faster workers with higher probability. Let $p_i = \hat{\mu}_i / (\sum_{i \leq n} \hat{\mu}_i)$. The proportional sampling procedure samples a worker from a multinomial distribution (p_1, p_2, \dots, p_n) . When the $\hat{\mu}_i$'s are accurate, workers behave like independent queues under proportional sampling with high probability that the maximum queue length is $O(\log n)$.

2. Power-of-two-choices with SQ(2). We integrate PoT techniques to further reduce the maximum queue length, i.e., we use PSS to choose two workers and place the new job to the better one. As discussed earlier, we can use SQ(2) or LL(2) policy. Rosella uses SQ(2) since it avoids using slower servers until too many jobs are waiting at the faster server:

EXAMPLE 3. A system consists of $n = \mu + 1$ worker, where $\mu \gg 1$ is an integer. Worker 1's processing rate is μ and the other servers' processing rate is 1. The total processing rate is 2μ , and the first server is substantially faster. The arrival rate of the jobs is 1.5μ .

The probability that worker 1 is chosen as a candidate is $1 - (\frac{1}{2})^2 = \frac{3}{4}$. When worker 1 is chosen as a candidate, it will pick up the new job if it has less than $\mu - 1$ jobs because the expected processing time for the other workers is at least 1 (even assuming the other candidate's queue is empty), whereas the expected processing time of worker 1 is < 1 when it has less than $\mu - 1$ jobs.

Assume that system starts with empty queues at time 0. In the beginning, the arrival rate to worker 1 is $1.5\mu \times \frac{3}{4} = \frac{9}{8}\mu$ while its processing rate is μ . Thus, the queue quickly builds up until its length hits $\mu - 1$. The queue will not shrink much afterward because as worker 1's queue decreases, worker 1 will attempt to pick up more jobs. Thus, in the stationary state, the length of queue 1 is around $\mu - 1$, and the expected waiting time for a job at worker 1 is $(\mu - 1 + 1)/\mu = 1$, which is as slow as the other slow servers.

In general, more jobs will be congested at the faster workers; all the workers could be as slow as the slowest server.

In the SQ(2) policy, however, slower workers will be utilized before faster servers become too full, alleviating the congestion problem.

3.2 Performance learner

The performance learner, which operates in the background, continuously maintains current estimates of each worker's processing power. It takes the estimate of λ as input and uses it to determine how often to communicate with the workers. The performance learner actively generates new jobs and assigns them to the workers (see LEARNER-DISPATCHER in Figure 6). The jobs serve as benchmarks to estimate the workers' processing powers.

Our system will generate the benchmark jobs according to a Poisson process with parameter $c_0(\bar{\mu} - \hat{\lambda})$, where $\bar{\mu}$ is the minimum guaranteed service throughput, $\hat{\lambda}$ is the estimate of

PPOT-SCHEDULING-POLICY(s_i)

- 1 $\triangleright s_i$ is the i -th job.
- 2 Let $p_i = \frac{\hat{\mu}_i}{\sum_{i \leq n} \hat{\mu}_i}$
- 3 Let $\vec{p} = (p_1, \dots, p_n)$.
- 4 $j_1, j_2 \leftarrow \text{multinomial}(\vec{p})$.
- 5 \triangleright let q_i be the length of queue i .
- 6 $j^* = \arg \min_{j \in \{j_1, j_2\}} \{q_j\}$.
- 7 \triangleright place the job at the j^* -th server.

Figure 5: Pseudocode for our proportional-sampling+PoT scheduling policy.

arrival rates, and c_0 is a small constant (say 0.1). Generating jobs at this frequency ensures that we optimally monitor all resources in the cluster while not jamming the system and slowing down the processing of other jobs. The benchmark jobs have low priorities, which will not be executed if other "real" jobs are waiting in the worker.

Choosing benchmark jobs. The benchmark jobs shall resemble recent workloads. For example, they can be replicates of the most recent queries at the frontend.

Learning. When worker i completes computation of a job, it will communicate with the performance learner to update its estimate $\hat{\mu}_i$ (see LEARNER-AGGREGATE in Figure 6). The estimate is based on computing the average processing time of the last L jobs, where $L = \Theta(\frac{\log(1/n)}{(1-\alpha)^2})$, and $\hat{\alpha} = \hat{\lambda}/\bar{\mu}$ is the estimated load ratio. The historical window length depends on the load ratio α and total number of jobs n for the following reasons: When α is small, there are sufficient residual compute resources so we can afford to have sloppy estimates. Therefore, the size of the historical window shrinks when α decreases. There is also a dependency on $\log 1/n$ because we need to use the standard Chernoff/union bound techniques to argue that all estimates are in reasonable quality (see Section 4 for the analysis).

When a worker is small, it may take time to collect the statistics over its most recent L tasks. Therefore, we set a waiting time cut-off, i.e., if we cannot estimate μ_i in $(1 + \epsilon)L/\mu^*$ time (the variables are defined in the pseudocode), we set the estimate at 0, effectively treating the small worker as dead.

3.3 The arrival estimator

This component estimates λ , using the mean interarrival time for the last S jobs as the estimation of $1/\lambda$. Here, S is a hyperparameter. When S is large, the estimate of λ is more accurate, but the system reacts more slowly to the change of worker speeds. When S is small, of the estimate of λ is less accurate, but the system reacts more rapidly to the environment changes.

4. ANALYSIS OF THE ALGORITHMS

LEARNER-DISPATCHER

- 1 ▷ this procedure dispatches benchmark jobs to workers
- 2 Sample $t_i \sim \text{Poisson}(0.1(\bar{\mu} - \hat{\lambda}))$.
- 3 at time t_i :
- 4 $j \leftarrow \text{Uniform}([n])$.
- 5 assign a low priority job to worker j .

LEARNER-AGGREGATE(worker i)

- 1 ▷ When a worker completes a job,
- 2 ▷ it invokes this function to communicate with
- 3 ▷ performance learner
- 4 $\hat{\alpha} \leftarrow \hat{\lambda}/\bar{\mu}$, $\epsilon = \frac{3}{10}(1 - \alpha)$, $\mu^* = (1 - \hat{\alpha})/10$.
- 5 $L \leftarrow \frac{c_2}{\epsilon^2} \log(1/n)$ for some constant c_1 .
- 6 Let \hat{q}_i be the average processing time
- 7 for the most recent L jobs
- 8 **if** cannot measure \hat{q}_i in $(1 + \epsilon)L/\mu^*$ time,
- 9 ▷ the workers too slow
- 10 **then**
- 11 $\hat{\mu}_i = 0$.
- 12 **else**
- 13 $\hat{\mu}_i = (1 - \epsilon)1/\hat{q}_i$
- 14 Report $\hat{\mu}_i$ to the performance learner

Figure 6: Pseudocode for the performance learner.

Our model. We consider a distributed system that consists of n workers/servers, each connected to a scheduler. Jobs arriving to the scheduler may contain one or more tasks. When a new job arrives, the scheduler can probe a certain number of workers and decide how the tasks should be assigned to the workers based on their queue length. For simplicity, our theoretical model focuses on the case of one job containing one task (but our evaluation will consider the general case).

The arrivals of jobs follows a Poisson distribution with parameter λ . Processing/compute power of the workers is heterogeneous. The service time for a job assigned to worker i follows an exponential distribution with parameter μ_i .

Let $\mu = \sum_{i \leq n} \mu_i$ be the system's total processing power, and $\alpha = \lambda/\mu$ be the system's load ratio.

Both μ_i and λ can change over time to reflect volatility in the system. $\bar{\mu}$, which is always larger than the job arrival rate.

Discrete-time counterpart. We use a standard way to couple our continuous time model with a discrete time model [24]. The discrete time model proceeds in rounds. One of the following events occurs in each round: (i) With probability $\lambda/(\lambda + \mu)$, one new job arrives, and (ii) With probability $\mu_i/(\lambda + \mu)$, one processing event happens at worker i as follows: if the worker's queue contains one or more jobs, the the oldest job is processed first. Otherwise, nothing happens.

One round in the discrete time model corresponds to a “jump” event in the continuous time model. Because we have coupled models (e.g., a convergence result for one often implies a similar result for the other), our analysis can switch between them to deliver an intuitive analysis.

Main results. Our system is highly efficient and scalable:

Result 1. Maximum load. With high probability the maximum queue length is $O(\log \log n)$ at the stationary distribution, generalizing existing PoT results. *Result 2. Learning speed.* The time it takes to learn all the parameters μ_i is $O\left(\frac{\log(1/n)}{(1-\alpha)^2}\right)$. Thus, when the number of workers doubles, it takes only a constant amount of additional time to learn the system. *Result 3. Convergence time.* When the system has reliable estimates of the processing powers, it takes additional $O(1)$ time to converge to the stationary distribution.

Interpreting the results. Consider the “life cycle” of Rosella. At t_1 , Rosella is in stationary distribution. Here, we may apply result 1: the maximum load at t_1 is $O(\log \log n)$ with high probability. At $t_2 > t_1$, the system experiences a shock (the processing power of a large number of workers get changed) and the estimates are no longer correct. Rosella then needs to re-learn the new worker speeds. Result 2 states that the learning time is $O(\log 1/n)$. Let $t_3 = t_2 + O(\log 1/n)$ be the time the system re-learns the worker speeds. At this time, there could be backlogs during the learning (between time t_2 and t_3) because the system has been using inaccurate estimates. So we need to wait more time for Rosella to return to normal. Result 3 states that it takes $O(1)$ time to clear up backlogs.

Notations. We use u, v to represent vectors, where u_i (v_i) represents the i -th entry of u (v). \mathbf{u} and \mathbf{v} are random vectors. We refer to the process produced by Rosella as a PPOt process (proportional sampling + PoT). We denote a PPOt process as $\{\mathbf{u}(t)\}_t$. Let the stationary distribution of a PPOt be \mathbf{u}_π . Abusing the notation, let $\{\mathbf{u}_\pi(t)\}$ be a PPOt process that starts with stationary distribution. Below, we explain our analysis of the three key results. We start with result 2 because the analysis is more complex, followed by results 1 and 3.

4.1 The “recovery time” of the PPOt process

Assuming that the system starts with an arbitrary state (e.g., recently experienced a shock) and our algorithm knows the exact μ_i 's, Section 4.1 bounds the time needed for a PPOt process to converge to the stationary distribution.

Defining recovery time. One way to define recovery time is the mixing time, i.e., the time it takes for the load distribution to be statistically-close to the stationary distribution, where the statistical distance between two random vectors \mathbf{v} and \mathbf{u} is defined as $\|\mathbf{u} - \mathbf{v}\|_{\text{TV}} = \sum_w \|\Pr[\mathbf{u} = w] - \Pr[\mathbf{v} = w]\|_1$. The example below shows the statistical distance is an unsuitable metrics.

EXAMPLE 4. Consider two systems whose loads are represented by \mathbf{u} and \mathbf{v} . Let $\mathbf{u}_1 = 1$ and $\mathbf{v}_1 = 0$ (i.e.,

worker 1 in \mathbf{u} always has 1 task while it always has 0 task in \mathbf{v}). The rest workers have i.i.d. distribution. Intuitively, the distributions of two systems should be close because they differ only on the first servers. But $\|\mathbf{u} - \mathbf{v}\|_{TV}$ is 1 because their supports are disjoint (coming from the fact \mathbf{u}_1 and \mathbf{v}_1 never agree).

We introduce a new metric to better capture the closeness between two systems. Recall that the ℓ_0 -distance two vectors is $\|u - v\|_0 = \frac{1}{n} \sum_{i=1}^n I(u_i \neq v_i)$, where $I(\cdot)$ is an indicator function that sets to one if and only if its argument is true. We have

DEFINITION 1 (ℓ_0 -DISTANCE BETWEEN LOADS).

The ℓ_0 -distance between two random vectors \mathbf{u} and \mathbf{v} , namely $\mathbf{D}(\mathbf{u}, \mathbf{v})$, is at most ϵ if there is a way to couple \mathbf{u} and \mathbf{v} such that $\mathbb{E}[\|\mathbf{u} - \mathbf{v}\|_0] \leq \epsilon$.

This definition measures only the number of servers that have different loads in two systems. In Example 4, the statistical-distance between them is 1, but the ℓ_0 distance is $\frac{1}{n} \rightarrow 0$, as n grows, thus properly capturing the fact that two systems are close.

Let $\mathbf{v}(t)$ be the load vector at time t of a PPOt process that starts at an arbitrary state with $C_{\max} = \|\mathbf{v}(0)\|_{\infty}$.

DEFINITION 2 (RECOVERY TIME). Using the notations above, the recovery time $T(\mathbf{v}, \epsilon)$ of a PPOt process that starts with \mathbf{v} is $T(\mathbf{v}, \epsilon) = \min_t \{\mathbf{D}(\mathbf{v}(t), \mathbf{u}_{\pi}(t)) \leq \epsilon\}$.

Intuitively, after $T(\mathbf{v}, \epsilon)$ time, only ϵ -portion of the workers are inconsistent with the stationary distribution. The rest workers all recovered. We have

PROPOSITION 1. Using the notations above, the recovery time $T(\mathbf{v}, \epsilon) = O(C_{\max} \log(1/\epsilon))$, i.e., it does not depend on the size n of the system.

For simplicity, we assume that α is suitably small. Techniques developed in our analysis can be generalized for arbitrary α . Proving Proposition 1 consists of two major steps:

Step 1. A conservative estimate of the stationary distribution. Let $\{\mathbf{v}(t)\}_t$ be an arbitrary PPOt process. Let f_i be the PDF for the marginal distribution of worker i at the stationary state. The tail of f_i decays with at least exponential rate (i.e., $f_i(j) \leq \rho f_i(j+1)$ for some $\rho < 1$). This is because the PPOt algorithm is at least as good as the proportional sampling algorithm. Using a Markov inequality, we have:

LEMMA 1. Let ϵ be an arbitrary constant and \mathbf{u}_{π} be the stationary distribution. Let $\mathbf{u}_{\pi,i}$ represent the i -th coordinate of \mathbf{u}_{π} . There exists a constant η (that depends only on ϵ) such that that: $\Pr \left[\sum_{i \leq n} I(\mathbf{u}_{\pi,i} \leq \eta) \leq (1 - \epsilon)n \right] \geq 1 - \epsilon$.

Lemma 1 implies that at the stationary distribution, most workers will have constant queue length.

We also observe that $\|\mathbf{v}(t) - \mathbf{u}_{\pi}(t)\|_0$ is *not* monotonically decreasing and thus it is remarkably difficult to directly track this quantity. Thus, we focus on the evolution of $\|\mathbf{v}(t) - \mathbf{u}_{\pi}(t)\|_1$:

LEMMA 2. Using the notations above, we have $\|\mathbf{v}(t) - \mathbf{u}_{\pi}(t)\|_1 \geq \|\mathbf{v}(t) - \mathbf{u}_{\pi}(t)\|_0$. Moreover, $\|\mathbf{v}(t) - \mathbf{u}_{\pi}(t)\|_1$ is monotonically decreasing regardless of the initial state $\mathbf{v}(0)$.

The monotone property is a known result and can be proved by a simple combinatorial analysis. See also [23].

Step 2. $\|\mathbf{v}(t) - \mathbf{u}_{\pi}(t)\|_1$ shrinks quickly. We next show that $\|\mathbf{v}(t) - \mathbf{u}_{\pi}(t)\|_1$ has exponential decay. We need to circumvent two key challenges: (i) The discrepancies in loads at the same workers could increase, i.e., it is *not true* that $|\mathbf{v}_i(t) - \mathbf{u}_{\pi,i}(t)| \leq |\mathbf{v}_i(t+1) - \mathbf{u}_{\pi,i}(t+1)|$. Therefore, we cannot focus on individual workers only. (ii) The loads of different workers are correlated.

Our key idea is to identify a group of events that occur sufficiently often, and when such an event occurs, $\|\mathbf{v}(t) - \mathbf{u}_{\pi}(t)\|_1$ strictly decreases.

A deletion event at time t at workers i is a *good deletion event* if worker i is empty in one of $\{\mathbf{v}(t), \mathbf{u}_{\pi}(t)\}$ and non-empty in the other one. A good deletion event has no effect on, for example, \mathbf{v}_i but $\mathbf{u}_{\pi,i}$ is decremented by one. After the deletion event, we have $\|\mathbf{u}_{\pi}(t+1) - \mathbf{v}(t+1)\|_1$ is decremented by 1. The frequency of good deletion events is characterized by the following lemma.

LEMMA 3. Using the above notations, there exists a constant C such that with constant probability,

$$\|\mathbf{v}(t+C) - \mathbf{u}_{\pi}(t+C)\|_1 \leq c_1 \|\mathbf{u}_{\pi}(t) - \mathbf{v}(t)\|_1 \quad (1)$$

Outline of the proof. When the loads of workers i are different in two processes, each loads perform a “left-drifting random walk” with a left bound 0. With a constant probability, within $\Theta(1)$ steps, one walk will hit zero first, and a good deletion event will occur. We next need to count the number of workers with different loads at t , i.e., $\|\mathbf{v}(t) - \mathbf{u}_{\pi}(t)\|_0$. We observe that with high probability $\|\mathbf{v}(t) - \mathbf{u}_{\pi}(t)\|_0 = \Theta(\|\mathbf{v}(t) - \mathbf{u}_{\pi}(t)\|_1)$. When we have large number of excessively long queues, ℓ_0 -norm of a vector could be much smaller than the ℓ_1 -norm. But having excessive long queue is a rare event; we can use this intuition to show that ℓ_1 -norm and ℓ_0 -norm of $\mathbf{v}(t) - \mathbf{u}_{\pi}(t)$ are in the same order.

Lemma 3 and the fact that $\|\mathbf{v}(t) - \mathbf{u}_{\pi}(t)\|_0 = \Theta(\|\mathbf{v}(t) - \mathbf{u}_{\pi}(t)\|_1)$ imply $\|\mathbf{v}(t) - \mathbf{u}_{\pi}(t)\|_0$ shrinks by a constant portion in $O(1)$ time. Proposition 1 the follows.

4.2 Stationary distribution of a PPOt process

Using the framework developed in [22, 23], we analyze the stationary distribution based on an ansatz.

An ansatz. Consider the load balancing system described above that operates under the SQ(2)-policy, with $\alpha < 1$.

When $n \rightarrow \infty$, there is a unique equilibrium distribution. Moreover, under this distribution, any finite number of queues are independent¹.

Our main result is that the marginal stationary distribution of all the workers is the same, regardless of their processing power.

Consider the first queue and sample its processing power from a power law distribution. The potential arrival process at queue 1 consists of jobs that have worker 1 as one of the choices. At any time t , let the empirical distribution of queues $2, \dots, n$ be denoted by $\mu^n(t)$, i.e., $\mu_k^n(t)$ is the weighted portion of workers having load k . Let μ_π^n denote this measure when the n -queue system is in equilibrium.

By the ansatz, μ_π^n converges to a fixed limiting measure μ_π that is independent of the size of the first queue, i.e., as $n \rightarrow \infty$, the background distribution μ_π is independent of queue 1. In fact, the actual arrival at queue 1 is specified by a state dependent Poisson process of rate λ_K when the queue size is k . Let $M_k = \sum_{j \geq k} \mu_{\pi,j}$. One can see that $\lambda_k = \alpha \left(\frac{M_k^2 - M_{k-1}^2}{M_k - M_{k+1}} \right)$. A fixed point solution is when $\mu_{\pi,k} = \alpha \frac{2^k - 1}{2^{k-1}}$. This implies:

LEMMA 4. Consider our PPoT process at the stationary distribution, with high probability that the maximum queue is in $O(\log \log n)$.

4.3 Learning the parameters

Wlog, assume that the average service rate of the workers is 1. The total amount of unused compute power is $(1 - \alpha)n$, where α is the load ratio. We further assume α is known because this can be easily estimated.

Performance goal and handling excessively slow servers. Our estimation procedure aims to efficiently estimate all μ_i within a short period but doing so is impossible for excessively slow workers, i.e., waiting for one job to complete is unacceptable. Our crucial observation is that if a server’s processing power is too weak, we can safely ignore them (i.e., set the estimate to be 0). Specifically, we set $\epsilon = \frac{3}{10}(1 - \alpha)$ so that $(1 - \epsilon)^3 \geq \frac{10\alpha}{9 + \alpha}$. We need wait only for $(1 + \epsilon)L/\mu$ time. If the estimation takes longer, we stop and set the estimate to 0.

Using standard Chernoff bound arguments, we have:

LEMMA 5. LEARNER-AGGREGATE(worker i) in Fig. 6 possesses the following properties: (i) For any workers i such that $\mu_i \leq (1 - \epsilon)\frac{1-\alpha}{10}$, our estimate will be $\hat{\mu}_i = 0$ (i.e., all slow servers will be discarded); (ii) For any workers i such that $\mu_i \geq \frac{1-\alpha}{10}$, our estimate needs to be an underestimate and guarantees ϵ -multiplicative error, i.e., $(1 - \epsilon)\mu_i \leq \hat{\mu}_i \leq \mu_i$; and (iii) For any workers i such that $(1 - \epsilon)\frac{1-\alpha}{10} \leq \mu_i \leq \frac{1-\alpha}{10}$, we have either $\hat{\mu}_i = 0$ or $(1 - \epsilon)\mu_i \leq \hat{\mu}_i \leq \mu_i m$ i.e., it could be discarded; but if it is kept, our estimate will be reliable.

¹Interested readers could also generalize the analysis in [23] to prove the ansatz.

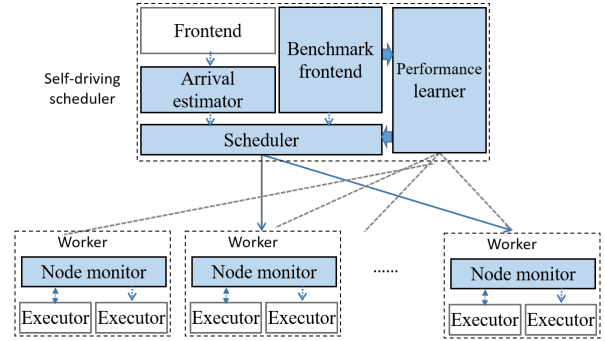


Figure 7: Implementation of our system.

Reliable estimates imply an efficient system. Finally, we have (see the technical report for the analysis [25]):

LEMMA 6. Consider a PPoT system in which the algorithm uses estimates $\hat{\mu}_i$ that satisfy the aforementioned properties. We have: (i) The PPoT process is stationary, and (ii) With high probability the maximum queue is $O(\log \log n)$ and the convergence time is $O(1)$.

5. IMPLEMENTATION

We implement our key modules (arrival estimator, scheduling policy, and performance learner) in Sparrow, a distributed scheduling system designed to process homogeneous jobs for homogenous schedulers [7].

Original Sparrow. Sparrow’s scheduling algorithm leverages power-of-two-choices, batching, and late-binding. One or multiple frontend boxes controls many backend workers. Each frontend box has a frontend module serving as the entry-point of the jobs/tasks.² The frontends interact with the schedulers, which dispatch jobs to the backend workers. Each backend worker consists of two components: a node monitor module that federates resource usages and communications with the frontends, and an executor that processes the tasks. The executor can be a Spark executor or any generic executors that implement proper interfaces to interact with node monitor. Thrift handles the communication between components.

Our implementation. See Figure 7. To enable learning, we integrate our modules as follows.

At the frontend: An arrival rate estimator that estimates the intensity/load of the system A benchmark (fake job) frontend that dispatches jobs uniformly for the purpose of estimating worker speed A performance learner that continuously estimates worker speed.

At the backend: Each node monitor maintains two separate queues: one queue is responsible for holding the “real” jobs and the other is responsible for holding the “fake” (benchmark) jobs. When a benchmark or real task completes, the

²We follow Sparrow’s convention to let a task be the minimum compute unit in the system, and one job contains one or more tasks.

node monitor reports an updated estimation of worker speed to the performance learner.

Distributed scheduler. When there are multiple schedulers, they need only synchronize the estimates of worker speeds regularly. The communication is also done through Thrift. When there are multiple schedulers running, excessive amount of benchmark jobs (from different frontends) could be sent to the node monitor. Setting priorities of the queues and implementing throttling ensures the benchmark jobs will not adversarially affect the system.

6. EVALUATION

We perform our experiments in AWS clusters. We examine Rosella for both real loads (TPC-H) and synthetic loads. Synthetic loads allow us to create extreme environments to understand the robustness of different systems.

The baselines we examine include: (i) uniform random: when a new job arrives, the scheduler uniformly chooses a backend worker, (ii) Power-of-two-choices, (iii) Sparrow [7], (iv) PSS+Learning: it continuously estimates worker speeds and uses the estimates to run the proportional sampling algorithm, and (v) Multi-armed bandit: when a new job arrives, with η probability, we uniformly choose a worker to serve the job. With $1 - \eta$ probability, we use PSS+PoT³. We examine $\eta \in \{0.2, 0.3\}$, and (vi) Halo [10]: an heterogeneity-aware scheduler that assumes the knowledge of worker speeds. This will only be briefly examined in synthetic loads and we shall see its performance gain is limited even it has accurate knowledge of λ and μ_i 's.

6.1 TPC-H Workload

The TPC-H benchmark [26] is representative of ad-hoc queries that have low latency requirements. Our experiments are similar to those in [7]. We use two query ids q3 and q6 in our experiments.

Setup. We evaluate schedulers' performance on TPC-H benchmark on a cluster of 31 memory-optimized EC2 instances (m2.4xlarge, with 64G memory) consisting of one scheduler and 30 workers.

Execution workflow. The TPC-H workload is submitted to Shark, which compiles the queries into Spark stages (also referred to as requests) and waits for scheduling. Rosella resides inside Spark and controls the scheduling policy. Each stage corresponds to a job, which consists of multiple tasks. The benchmark consists of constrained (total # of tasks is 2k) and unconstrained tasks (total # tasks is more than 30k). A constrained task needs to be executed at a specific backend so schedulers do not have any freedom (i.e., the PPOt scheduling policy is disabled for constrained tasks). Unconstrained tasks can be executed in any worker.

Running the benchmark takes approximately 60 minutes. We report the result of the 40 minutes in the middle

³No existing system directly uses this baseline but since this is an intuitive design, we need to understand its performance.

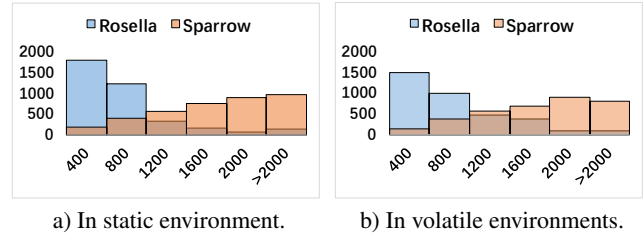


Figure 8: Distribution of response time for unconstrained requests.

of execution (up to the point 30k tasks or 6.2k stages are completed).

Controlling worker speed. While all EC2 instances are of the same type, we modify the executor in Spark to slow down a worker k times: When a worker receives a task, it executes the task and records the execution time T . After completing the task, the worker holds the task $(k - 1)T$ more time and then informs to the node monitor that the task is completed. The worker speeds (μ 's) are from the set $\{0.01, 0.04, \dots, 0.81\}$ to mimic heterogeneous environments. The choice of workloads are not critical. Other workloads also exhibit similar qualitative behaviors.

Integration with late-binding. Rosella is compatible with late binding so this technique is also integrated into Rosella.

Baselines. The baselines we consider include Sparrow, Power-of-two-choices, and Multi-armed bandit. Other prior baselines (e.g., uniform random, per task sampling, or batch sampling) are not included because their performances are significantly worse.

Response time under static environment. We first consider the case, where worker speeds are known and do not change over time. The *response time* of a job is the time between the job arrives at the scheduler and the time when the last task in the job is executed.

Figure 8a shows the response time distributions under Sparrow and Rosella. Rosella's distribution decays exponentially before 2,000ms (thus, most jobs complete before 2,000ms) whereas Sparrow's distribution is *monotonically increasing*, with a much larger portion of jobs that cannot be completed in 2,000ms.

We next examine all the baselines. See the Figure 9a. Rosella's performance is uniformly better than all other baselines in both q3 and q6. Multi-armed bandit algorithm has the worst performance. We can also see the breakdown of performance gains. Introduction of PSS helps the system to outperform Sparrow. When PoT and late-binding techniques are introduced, the performance continues to improve. The average response time for Sparrow is 1,901 while the average response time for Rosella is 675, corresponding to 65% of improvement.

Evolving worker speed. We next consider a system, in which the worker speeds evolve over time. We randomly permute the worker speeds every two minutes to focus on

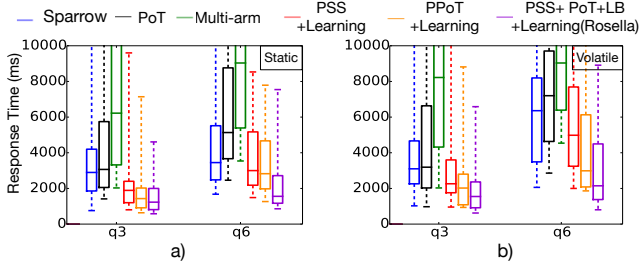


Figure 9: Response time (in ms) for TPC-H queries. The 5th, 25th, 50th, 75th and 95th percentiles are presented. The load is 0.8.

the “transient behaviors” of schedulers (i.e., their behaviors in the short time window right after the shock). This setup also ensures that the total throughput remains unchanged over time so that we can focus on the learning behaviors (instead of the overload behaviors) of the system.

Figure 8b shows a comparison between Rosella and Sparrow. Again, a significant portion of jobs at Sparrow cannot be completed with 2,000 seconds. The performance of Rosella degrades (compared to the static setting) because it needs to continuously learn the new worker speeds and adjust its scheduling policy. Sparrow’s performance does not degrade because Sparrow’s policy is already oblivious to the worker speeds, and therefore changing the policy will not further “harm” sparrow.

Figure 9b shows the performance of Rosella and all baselines. Rosella has the best performance. PSS+Learning and PPoT+Learning all have better performance than Sparrow, PoT, or Multi-armed bandit. The algorithms that use learning (multi-armed, PSS+Learning, PPoT+Learning, Rosella) all have degraded performance compared to the static setting. The algorithms that do not learn (Sparrow and PoT) do not degrade for the same reason discussed above.

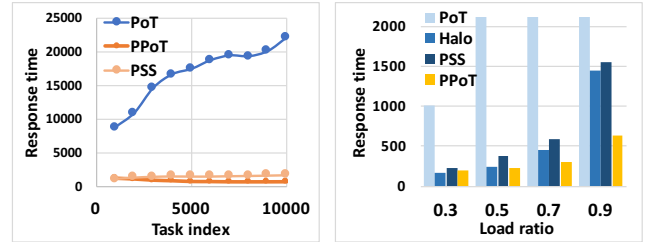
6.2 Synthetic workloads

Next, we consider synthetic workloads. Tasks are “sleep” tasks (i.e., after receiving a new task, the worker will sleep for a period).

Setup. A scheduler controls 15 workers to mimic typical computing environments in industrial and research labs. The processing time (sleep time) of i -th task processed by the j -th worker is τ_i/μ_j , where each τ_i is independently sampled from an exponential distribution with mean 100ms. μ_j controls the speed of worker j . Our experiments control the evolution of $\{\mu_j\}_j$ to produce heterogeneous and volatile computing environments.

Heterogeneity. We first assume that the worker speeds μ_j are all known. The worker speeds are independently sampled from a Zipf’s distribution where there is a small number of powerful servers.

1. *Significant degradation in PoT and Random.* See Fig-



a) PoT’s response time is b) Response times under different non-stationary loads

Figure 10: Response times for different schedulers when the worker speeds are known.

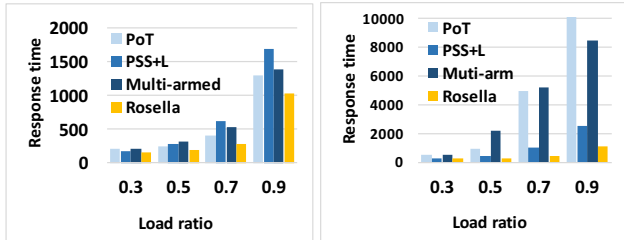
ure 10a. The x -axis represents the indices of the jobs (i.e., a job with a large index means it arrives late). When the workload is large ($\lambda/\mu = 0.9$), the PoT baseline has unbounded queue length/waiting times. The response time for uniform random policy grows too fast and is removed from the chart. The average response time grows as more jobs arrive while the PSS or PPoT algorithms’ response times stay stationary.

2. *Benefits across all loads.* We next examine the schedulers’ performance under different loads. See Figure 10b. The x -axis represents the load ratio. The y -axis represents the response time. PPoT has the best performance across all loads. Its performance improvements are moderate when the loads are low and become significant when the loads are high. Also, the moderate performance difference between Halo and PSS suggests that Halo has a limited benefit.

Full-fledged execution. We next examine the setting with changes in worker speeds. We reuse the random permutation model described in Section 6.1. Specifically, the worker speeds always come from the same set, and the speeds are randomly permuted every minute. We consider two speed sets $S_1 = \{0.2, 0.3, \dots, 1.6\}$ and $S_2 = \{0.15, 0.15, 0.15, 0.15, 0.15, 0.2, 0.3, 0.4, 0.5, 0.6, 1, 1, 1, 2, 2\}$. S_2 represents a more heterogeneous setting. The workloads are chosen arbitrarily; other workloads exhibit similar qualitative behaviors. Schedulers examined include PoT, PSS+Learning (with fixed sliding window), multi-armed bandit, and Rosella.

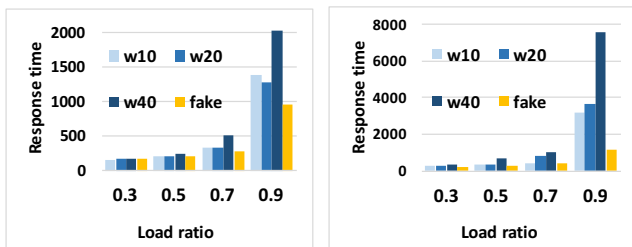
Determining sliding window size. The sliding window used to compute worker speed needs to be dynamic (see Section 4), e.g., we use short windows for small loads while using long windows for large loads. While the theoretical results suggest that a sliding window of size $c/(1-\alpha)^3$ is asymptotically optimal, in practice, this window size is too conservative. Setting it to be $c/(1-\alpha)$ achieves the best performance in practice.

Figure 11 shows the result (i.e., Figure 11a uses S_1 as the worker speed set and Figure 11b uses S_2). We observe that (i) Rosella has the best performance across all load ratios for both loads. When the load ratio is large, the performance gap between ours and the baselines are more



a) Worker speeds are from S_1 b) Worker speeds are from S_2 (less heterogeneous). (more heterogeneous).

Figure 11: Performance of schedulers when worker speed changes.



a) The impact of fake jobs b) The impact of fake jobs (using S_1). (using S_2)

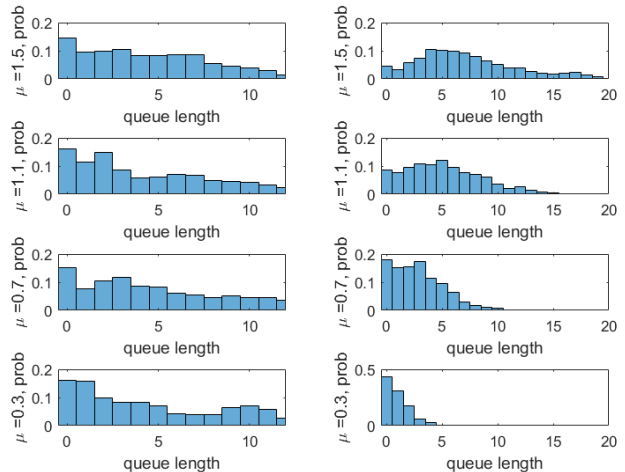
Figure 12: Impact of using fake jobs in Rosella.

pronounced. When the environment is more heterogeneous (S_2), the performance gap also increases.

The impact of introducing fake jobs. We next examine the role of fake jobs in Rosella. We disable the production of fake jobs, and examine different dynamic window sizes (i.e., try different constants c for the window sizes $c/(1-\alpha)$). We aim to understand whether adjusting the window size can achieve the same performance without fake jobs.

We use the same setup (i.e., we randomly permute two worker speed sets S_1 and S_2 every minute.). Our baselines are PSS+PoT+Learning with different sliding window sizes. Recall that the sliding window size is $c/(1-\alpha)$. We examine $c = \{10, 20, 30, 40\}$ (e.g., w10 refers to setting $c = 10$). See Figure 12 for the result. We observe that while having longer sliding windows improves estimation quality, it does not translate into improvement in processing time. On the other hand, using fake jobs consistently improves the response times under different loads for different worker speed sets. Similar to the above experiments, the improvement of using fake jobs becomes more pronounced when the load ratio is high, or when the worker speeds are highly heterogeneous.

SQ(2) vs. LL(2) policies. We examine the behaviors of SQ(2) and LL(2). The worker speed set is $\{0.2, \dots, 1.6\}$. The worker speeds do not change in this setting. We arbitrarily choose four workers with different speeds and plot the histograms of their queue lengths (normalized by the to-



a) Using SQ(2) policy. b) Using LL(2) policy.

Figure 13: Distribution of queue length using SQ(2) and LL(2) policies. From top to bottom: faster to slower workers.

tal number of jobs).

Figure 13a shows the result. The workers are sorted according to their speeds (e.g., the fastest worker is at the top).

1. *Stationary distribution of SQ(2).* Figure 13a shows that when we use SQ(2), the distributions of queue length for workers with different speed have the same distribution, confirming the theoretical results in Section 4.2.

2. *LL(2) prefers faster workers.* Comparing SQ(2) (Figure 13a) with LL(2) (Figure 13b), we see that LL(2) policy has a stronger preference of using faster workers even when their queues are excessively long. For example, the queue length of the faster worker is long tailed (top of Figure 13b), and is twice as long as the same worker in LL(2) (top of Figure 13a), whereas the slowest worker (bottom of Figure 13b) has a much shorter queue. Therefore, all workers in LL(2) will behave as slow as the slowest worker.

7. RELATED WORK

Schedulers. The job scheduling problem is widely studied in industry and academia. Mesos [27], YARN [28], and Omega [29] are production-strength schedulers that allocate resources at coarse granularity. Because in part they need to support complex operations, they sacrifice request granularity and thus usually do not work for latency-sensitive tasks/jobs. A significant effort is devoted to design schedulers that are fair, often at the cost of reduced efficiency [30, 31, 32].

Performance-optimized schedulers [12, 15, 33] use a different set of techniques. For example, the “shortest remaining processing time” policy prioritizes smaller jobs so that the average waiting time is optimized [12, 15, 14, 34].

These techniques are not applicable in our setting because our jobs are relatively homogeneous, and all jobs have low latency requirements. The so-called “late-binding” technique formally introduced in [7] also resembles an earlier technique developed by Dean [2]. Roughly speaking, the system may send the same requests to multiple workers but cancel the remaining outstanding requests while one of them is processed/completed. Ananta [35] is a layer-4 load-balancer that combines techniques in networking and distributed systems to refactor its functionality to meet scale, performance, and reliability requirements.

Distributed/decentralized schedulers focus on a system’s scalability and are often designed to minimize coordination/communication. Duet [36] is a distributed hybrid load balancer that fuses switch with the software load balancers. Apollo [37] is a coordinated scheduling framework that is suitable for executing “heavy jobs” (jobs requiring heavy resources).

Theory. Load balancing algorithms (sometimes under the name “balls-and-bins”) and power-of-two-choices in homogeneous systems have been extensively studied. See [18] for a comprehensive treatment of balls-and-bins, [11] for a survey of power-of-two-choices algorithms in discrete-time systems, and [17, 16] for more recent developments. For the continuous-time counterpart, see e.g., [13, 38] and references therein. Halo [10] provides an optimal scheduling policy in heterogeneous environments when the speed of the workers are known, and the scheduler can only probe one machine.

Mukhopadhyay and Mazumdar [39] studies a similar model to ours but they assume a constant number of worker types (the number of distinct μ_i ’s is $O(1)$), and their speeds are known. In their algorithm, they perform one proportional sampling at the group level (workers with the same speed are in the same group), and perform a PoT inside the group. This algorithm cannot be directly generalized to our setting.

Online estimation and change point detections are an extensively studied area [40, 41]. Stochastic optimization and exponential moving average [42] are widely used techniques to estimate the means of a sequence of i.i.d. random variables. For recent development in multi-armed bandit algorithms, see [19].

8. CONCLUSION

This paper introduces Rosella, a scalable self-driving scheduler for use in homogeneous and volatile environments (i.e., the processing powers of backend servers are different and evolve over time). Rosella achieves high throughput and low latencies by introducing two key modules: the scheduling policy leverages proportional sampling and power-of-two-choices to optimize the queue length, and the performance learner introduces benchmark/fake jobs and uses a dynamic sliding window to achieve optimal learning strategy. Rosella is implemented on real large computing clusters tested against both real and synthetic work-

loads. Our experiments show that Rosella significantly outperforms prior algorithms (e.g., Sparrow, PoT, and uniform), and is robust against various workloads. We conclude that our proposed scheduling policy and learning module have the potential to build a new generation of scalable, high-throughput, and latency-sensitive schedulers.

9. REFERENCES

- [1] Minlan Yu, Albert Greenberg, Dave Maltz, Jennifer Rexford, Lihua Yuan, Srikanth Kandula, and Changhoon Kim. Profiling network performance for multi-tier data center applications. In *Proceedings of the 8th USENIX Conference on Networked Systems Design and Implementation*, NSDI’11, pages 57–70, Berkeley, CA, USA, 2011. USENIX Association.
- [2] Jeffrey Dean and Luiz André Barroso. The tail at scale. *Commun. ACM*, 56(2):74–80, February 2013.
- [3] David Silver, Aja Huang, Chris J. Maddison, Arthur Guez, and et la. Sifre. Mastering the game of Go with deep neural networks and tree search. *Nature*, 529(7587):484–489, January 2016.
- [4] Amazon Web Services. Aws deep learning amis, 2017. <https://aws.amazon.com/amazon-ai/amis/>.
- [5] Amazon EC2. Amazon ec2 spot instances, 2017. <https://aws.amazon.com/ec2/spot/>.
- [6] Amazon EC2. Amazon ec2 t2 instances, 2017. <https://aws.amazon.com/ec2/instance-types/t2/>.
- [7] Kay Ousterhout, Patrick Wendell, Matei Zaharia, and Ion Stoica. Sparrow: distributed, low latency scheduling. In *Proceedings of the Twenty-Fourth ACM Symposium on Operating Systems Principles*, pages 69–84. ACM, 2013.
- [8] Martín Abadi, Ashish Agarwal, Paul Barham, Eugene Brevdo, Zhifeng Chen, Craig Citro, Greg S Corrado, Andy Davis, Jeffrey Dean, Matthieu Devin, et al. Tensorflow: Large-scale machine learning on heterogeneous distributed systems. *arXiv preprint arXiv:1603.04467*, 2016.
- [9] David Greenberg. *Building Applications on Mesos: Leveraging Resilient, Scalable, and Distributed Systems*. " O’Reilly Media, Inc.", 2015.
- [10] Anshul Gandhi, Xi Zhang, and Naman Mittal. Halo: Heterogeneity-aware load balancing. In *Modeling, Analysis and Simulation of Computer and Telecommunication Systems (MASCOTS), 2015 IEEE 23rd International Symposium on*, pages 242–251. IEEE, 2015.
- [11] Michael Mitzenmacher, Andréa W. Richa, and Ramesh Sitaraman. The power of two random choices: A survey of techniques and results. In *Handbook of Randomized Computing*, pages 255–312. Kluwer, 2000.
- [12] Donald R Smith. A new proof of the optimality of the shortest remaining processing time discipline. *Operations Research*, 26(1):197–199, 1978.
- [13] Colin McDiarmid and Malwina J. Luczak. On the power of two choices: Balls and bins in continuous time. *The Annals of Applied Probability*, 15(3):1733–1764, 2005.
- [14] Benjamin Moseley, Anirban Dasgupta, Ravi Kumar, and Tamás Sarlós. On scheduling in map-reduce and flow-shops. In *Proceedings of the twenty-third annual ACM symposium on Parallelism in algorithms and architectures*, pages 289–298. ACM, 2011.
- [15] Minghong Lin, Li Zhang, Adam Wierman, and Jian Tan. Joint optimization of overlapping phases in mapreduce. *Performance Evaluation*, 70(10):720–735, 2013.
- [16] Qiaomin Xie, Xiaobo Dong, Yi Lu, and Rayadurgam Srikant. Power of d choices for large-scale bin packing: A loss model. *ACM SIGMETRICS Performance Evaluation Review*, 43(1):321–334, 2015.
- [17] Lei Ying, R Srikant, and Xiaohan Kang. The power of slightly more than one sample in randomized load balancing. *Mathematics of Operations Research*, 2017.
- [18] Michael Mitzenmacher and Eli Upfal. *Probability and Computing: Randomized Algorithms and Probabilistic Analysis*. Cambridge University Press, New York, NY, USA, 2005.

- [19] Sébastien Bubeck, Nicolo Cesa-Bianchi, et al. Regret analysis of stochastic and nonstochastic multi-armed bandit problems. *Foundations and Trends® in Machine Learning*, 5(1):1–122, 2012.
- [20] Serguei Foss and Natalia Chernova. On the stability of a partially accessible multi-station queue with state-dependent routing. *Queueing Systems*, 29(1):55–73, 1998.
- [21] Robert D Foley and David R McDonald. Join the shortest queue: stability and exact asymptotics. *Annals of Applied Probability*, pages 569–607, 2001.
- [22] Maury Bramson, Yi Lu, and Balaji Prabhakar. Randomized load balancing with general service time distributions. In *ACM SIGMETRICS performance evaluation review*, volume 38, pages 275–286. ACM, 2010.
- [23] Maury Bramson, Yi Lu, and Balaji Prabhakar. Asymptotic independence of queues under randomized load balancing. *Queueing Systems*, 71(3):247–292, 2012.
- [24] Sheldon M Ross. *Introduction to probability models*. Academic press, 2014.
- [25] Anonymous (rosella.sigcomm@gmail.com). Rosella: a self-driving distributed scheduler for heterogeneous clusters. In *Technical Report (https://goo.gl/gKEF6R)*, January 2018.
- [26] The tpc benchmark h, 2017. <http://www.tpc.org/tpch/>.
- [27] Benjamin Hindman, Andy Konwinski, Matei Zaharia, Ali Ghodsi, Anthony D Joseph, Randy H Katz, Scott Shenker, and Ion Stoica. Mesos: A platform for fine-grained resource sharing in the data center. In *NSDI*, volume 11, pages 22–22, 2011.
- [28] A. C. Murthy. The next generation of apache mapreduce, 2017. <http://yahoohadoop.tumblr.com/post/98210076241/the-next-generation-of-apache-hadoop-mapreduce>.
- [29] Malte Schwarzkopf, Andy Konwinski, Michael Abd-El-Malek, and John Wilkes. Omega: flexible, scalable schedulers for large compute clusters. In *Proceedings of the 8th ACM European Conference on Computer Systems*, pages 351–364. ACM, 2013.
- [30] Michael Isard, Vijayan Prabhakaran, Jon Currey, Udi Wieder, Kunal Talwar, and Andrew Goldberg. Quincy: fair scheduling for distributed computing clusters. In *Proceedings of the ACM SIGOPS 22nd symposium on Operating systems principles*, pages 261–276. ACM, 2009.
- [31] Joel Wolf, Deepak Rajan, Kirsten Hildrum, Rohit Khandekar, Vibhore Kumar, Sujay Parekh, Kun-Lung Wu, et al. Flex: A slot allocation scheduling optimizer for mapreduce workloads. In *Proceedings of the ACM/IFIP/USENIX 11th International Conference on Middleware*, pages 1–20. Springer-Verlag, 2010.
- [32] Ali Ghodsi, Matei Zaharia, Benjamin Hindman, Andy Konwinski, Scott Shenker, and Ion Stoica. Dominant resource fairness: Fair allocation of multiple resource types. In *Nsdi*, volume 11, pages 24–24, 2011.
- [33] Kay Ousterhout, Aurojit Panda, Josh Rosen, Shivaram Venkataraman, Reynold Xin, Sylvia Ratnasamy, Scott Shenker, and Ion Stoica. The case for tiny tasks in compute clusters. In *HotOS*, volume 13, pages 14–14, 2013.
- [34] Yandong Wang, Jian Tan, Weikuan Yu, Li Zhang, Xiaoqiao Meng, and Xiaobing Li. Preemptive redcetask scheduling for fair and fast job completion. In *ICAC*, pages 279–289, 2013.
- [35] Parveen Patel, Deepak Bansal, Lihua Yuan, Ashwin Murthy, Albert Greenberg, David A Maltz, Randy Kern, Hemant Kumar, Marios Zikos, Hongyu Wu, et al. Ananta: cloud scale load balancing. In *ACM SIGCOMM Computer Communication Review*, volume 43, pages 207–218. ACM, 2013.
- [36] Rohan Gandhi, Hongqiang Harry Liu, Y Charlie Hu, Guohan Lu, Jitendra Padhye, Lihua Yuan, and Ming Zhang. Duet: Cloud scale load balancing with hardware and software. *ACM SIGCOMM Computer Communication Review*, 44(4):27–38, 2015.
- [37] Eric Boutin, Jaliya Ekanayake, Wei Lin, Bing Shi, Jingren Zhou, Zhengping Qian, Ming Wu, and Lidong Zhou. Apollo: Scalable and coordinated scheduling for cloud-scale computing. In *OSDI*, volume 14, pages 285–300, 2014.
- [38] Maury Bramson, Yi Lu, and Balaji Prabhakar. Randomized load balancing with general service time distributions. *SIGMETRICS Perform. Eval. Rev.*, 38(1):275–286, June 2010.
- [39] Arpan Mukhopadhyay and Ravi R Mazumdar. Analysis of randomized join-the-shortest-queue (jsq) schemes in large heterogeneous processor-sharing systems. *IEEE Transactions on Control of Network Systems*, 3(2):116–126, 2016.
- [40] H Vincent Poor. *An introduction to signal detection and estimation*. Springer Science & Business Media, 2013.
- [41] Alexander Tartakovsky, Igor Nikiforov, and Michele Basseville. *Sequential analysis: Hypothesis testing and changepoint detection*. CRC Press, 2014.
- [42] J Harold, G Kushner, and George Yin. Stochastic approximation and recursive algorithm and applications. *Application of Mathematics*, 35, 1997.